DEUTSCHES ELEKTRONEN-SYNCHROTRON DESY
DESY SR 89-04
September 1989

# Heating Effects of Monochromator Crystals at a High Intensity Wiggler Beamline

D. Degenhardt, R. Frahm, S. Joksch, G. Meyer
*Hamburger Synchrotronstrahlungslabor HASYLAB at DESY, Hamburg*
W. Jark
*Fritz-Haber-Institut der Max-Planck-Gesellschaft, Berlin*

Eigentum der DESY Bibliothek
Property library
Zugang
Accession 31. OKT. 1989
Leihfrist: 7 Tage
Loan period: 7 days

ISSN 0723-7979

NOTKESTRASSE 85 · 2 HAMBURG 52

DESY behält sich alle Rechte für den Fall der Schutzrechtserteilung und für die wirtschaftliche Verwertung der in diesem Bericht enthaltenen Informationen vor.

DESY reserves all rights for commercial use of information included in this report, especially in case of filing application for or grant of patents.

To be sure that your preprints are promptly included in the
HIGH ENERGY PHYSICS INDEX ,
send them to the following address ( if possible by air mail ) :

DESY
Bibliothek
Notkestrasse 85
2 Hamburg 52
Germany

DESY SR 89-04
September 1989

ISSN 0723-7979

# Heating effects of monochromator crystals at a high intensity wiggler beamline

Stefan Joksch, Detlev Degenhardt, Ronald Frahm, Gert Meyer
(Hamburger Synchrotronstrahlungslabor HASYLAB at DESY, Notkestr.85, D-2000 Hamburg 52, FRG)
Werner Jark [1]
(Fritz-Haber-Institut der Max-Planck-Gesellschaft, 1000 Berlin 33, FRG)

X-ray diffraction experiments on the first crystal of the ROEWI monochromator at HASYLAB were performed in order to study its reflection characteristics in dependence of thickness and cooling efficiency. Germanium (111) crystals with thicknesses of 5 mm and 1 mm were exposed to the beam from the wiggler (W1) at the storage ring DORIS. The results are compared with temperature measurements using an infrared camera and heat load calculations. For these calculations a one dimensional model as well as finite element methods are applied.

## 1. Introduction:

The use of x-ray wigglers and undulators as intense synchrotron radiation sources results in considerable heat load of the first optical components in the beamline [1]. In particular mirrors and single crystals essentially change their reflection characteristics under thermal load. The first crystal in a two-crystal monochromator will bend and expand which results in a loss of intensity in the monochromatic beam due to the change of the Bragg angle coupled with a decrease of energy resolution $\Delta E/E$. This effect becomes even more important if a high energy resolution is intended, for instance by use of reflections with high Miller-indices. The understanding and the reduction of these effects is of crucial importance for the operation of the next generation of dedicated storage rings with powerful insertion devices.

In the recent years the behaviour of optical components irradiated by intense x-radiation was investigated by infrared and interferometric [2,3] as well as x-ray diffraction methods [4,5]. Besides the question of best suited materials these investigations had been focused on effective cooling schemes [6,7,8].

The scope of the present work is to investigate the reflection curve of the first monochromator crystal of the ROEWI-monochromator at the 32-pole wiggler beamline W1 [9,10]. The three crystal configuration used in these experiments is described in detail in chapter 3. Two different cooling schemes were tested. The results are compared with temperature measurements using an infrared camera and heat load calculations. For these calculations a simple thermodynamic model presented in chapter 2 as well as finite element methods are applied.

[1] Present adress: Sincrotrone Trieste, Padriciano 99, I-34012 Trieste, Italy

to be published in Nucl. Instr. Meth. Vol. A, as
Proceedings of the SRI-89 Conference at Berkeley, USA

## 2. Theoretical

To calculate the heat load on a crystal irradiated by intense x-radiation the heat diffusion equation has to be solved. If no phase transition occurs it can be written as

$$c\rho\frac{\partial T(r,t)}{\partial t} = P(r,t) + \frac{\partial}{\partial r}(k(r)\frac{\partial T(r,t)}{\partial r}) \qquad (1)$$

with T(r,t) being the temperature as a function of space coordinate r and time t, c the specific heat, $\rho$ the density, k(r) the heat diffusion coefficient and P(r,t) the heat production term. This equation is usually solved by finite element methods. However, for an estimation of the maximum temperature rise in the crystal it is sufficient to solve the one dimensional equation, yielding in the steady state :

$$\frac{d}{dz}(k(z)\frac{dT(z)}{dz}) = -P(z) \qquad (2)$$

were z is the space coordinate perpendicular to the crystal surface. The heat production term P(z) results from the multiplication of the spectrum of the incident radiation $I_0(E)$ with the energy dependent photoelectric absorption coefficient $\mu(E)$ of the crystal. Assuming the material to be homogeneous it can be written as:

$$P(z) = \int dE I(z,E)\mu(E) = \int dE I_0(E)\mu(E)(1-R(E))sin\theta exp(-\mu(E)z) \qquad (3)$$

where R is the specular reflectivity at the surface of the first crystal, $\theta$ the angle of grazing incidence and E the energy. For typical monochromator crystals R becomes $< 10^{-6}$ for

angles of grazing incidence $\theta$ larger than the critical angle of total reflection $\theta_c$, which is for instance about 0.2 degree at a wavelength $\lambda$ of 0.15 nm and is even smaller than 1 degree for silicon crystals at $\lambda$ =0.5 nm .

Neglecting the temperature dependence of the heat diffusion coefficient and the heat radiated by the front side of the crystal equation (2) can be solved analytically. With the assumption that the temperature at the rear side of the crystal can be held at a constant value $T_0$ the temperature profile in the crystal is given by :

$$T(z)-T_0 = \int dE \frac{I_0(E)sin\theta exp(-\mu(E)z_0)}{k\mu(E)}[1-exp(-\mu(E)(z-z_0)-\mu(E)(z-z_0)exp(\mu(E)z_0)] \tag{4}$$

where $z_0$ is the thickness of the crystal. Under steady state conditions the heat flow through the rear side of the crystal is equal to the absorbed power in the whole crystal :

$$-k\frac{dT}{dz}|_{z=z_0} = \int dE I_0(E)sin\theta(1-exp(-\mu(E)z_0),$$

This offers a possibility to monitor the intensity of the beam incident on the first monochromator crystal by measuring both the flow rate and the temperature rise of the cooling liquid. Assuming $\mu z < 1$, which is valid for crystals of some millimeter thickness considering the whole spectrum emitted by the wiggler, we obtain for the surface temperature $T_s$:

$$\Delta T = T_s - T_0 = \int dE \frac{I_0(E)sin\theta\mu(E)z_0^2}{2k}, \tag{5}$$

For $\mu z \gg 1$ the depth dependence of the heat deposition can be neglected :

$$\Delta T = T_s - T_0 = \int dE \frac{I_0(E)sin\theta z_0}{k} \equiv \frac{P' z_0}{k}, \tag{6}$$

were P' is the power density. Equation (4) describes the temperature gradient inside the crystal. However, besides the thermal bending of the crystal [11, 12] especially this



temperature gradient is responsible for the intensity loss due to the change of the surface shape of the crystal. The change of the full width of half maximum (FWHM) $\omega^E$ of the reflection curve caused by thermal expansion can roughly be estimated [13] :

$$\omega^E = \alpha\Delta T tan\theta_B \tag{7}$$

with :

$$\alpha = \frac{3(1+2(c_{12}/c_{11}))}{(1+2(c_{12}/c_{11})+4(c_{44}/c_{11})}\alpha_0$$

for cubic (111) crystals, were $c_{ij}$ are the elastic strain constants and $\alpha_0$ the linear thermal expansion coefficient [14] and $\theta_B$ the Braggangle. The radius of curvature $R_c$ due to thermal bending of the crystal is described by [11]:

$$R_c = \frac{z_0}{\alpha\Delta T} \tag{8}$$

Taking into account equation (6) we obtain:

$$R_c = \frac{k}{P'\alpha} \tag{9}$$

Therefore, if $\mu$ z $\gg$ 1 the bending of the crystal does not depend on its thickness in contrast to the thermal expansion of the lattice. The bending of the crystal is combined with a lateral as well as depth-dependent change of the angle between the incident beam and the reflecting lattice planes resulting in a broadening of the rocking curve. The depth dependent contribution $\omega^D$ depends on the absorption depth $t_a$ [15] according to:

$$\omega^D = \frac{t_a}{Rsin\theta}. \tag{10}$$

The lateral change is

$$\omega^L = arctan(\frac{\Delta x}{R_c})$$

were $\Delta x$ is the vertical distance at the crystal surface. (11)

Calculations of the temperature profile T(z) using equation (4) were performed for germanium as well as silicon crystals placed in the ROEWI monochromator at the wiggler W1 at HASYLAB. The distance between source and crystal was 25.3 m. The low energy part (E < 5 keV) of the wiggler-spectrum is absorbed by carbon filters and beryllium windows placed in front of the first monochromator crystal. For the calculation we corrected the photon flux for the absorption losses in these filters of 0.2 mm (C) and 0.4 mm (Be) thickness (fig.1). In figure 2 the temperature profiles are shown, for 5 mm thick crystals, calculated for the parasitic (a) as well as the dedicated (b) shifts at DORIS, which are characterized by electron energies of 5.3 GeV and 3.5 GeV and maximum stored currents of 40 mA and 100 mA, respectively. The calculations were performed for 14 degree angle of grazing incidence corresponding to the Braggangle at ~8 keV. The temperature profiles show, that for the usual crystal thickness of 5 mm the heat load on the crystals is considerable high even at 3.5 GeV. In all cases the maximum temperature at the front surface is higher for germanium than for silicon crystals. This is partly due to the lower thermal conductivity of germanium. The comparision of the spectral power distribution of the wiggler W1 with the absorption coefficients of Ge and Si in figure 1 points to an enhancement of this effect. The K-absorption edge of Ge at $\lambda = 0.116$ nm coincides with the maximum of the spectral power distribution. The spectral power distribution we found also to be of extraordinary importance considering the behaviour of mirrors in intense wiggler beamlines [16].

Due to symmetry the finite element calculations were restricted to one quadrant of the crystal. Figure 3 shows the temperature distribution on the crystal surface for 5 and 1 mm thick germanium crystals calculated by the finite element method. In the calculations the geometry of the cooling system of the first crystal in the ROEWI monochromator is approximated. The calculated maximum temperatures at the crystal surface agree with the maximum temperature measured by infrared (IR)-camera (Table I). Both are larger than those obtained by means of the one dimensional model presented above, because the rear side of the crystal does not remain cool during the irradiation.

The surface deformation of a quadrant of a 5 mm thick crystal calculated with finite elements is shown in figure 4. The bending of the whole crystal as well as the surface bump due to the thermal expansion can be seen.



## 3. Diffraction experiments

The diffraction experiments were performed with three germanium crystals using the configuration sketched in figure 5. This experimental scheme allows the measurement of the reflection curve of the first crystal with high angular resolution in a small energy band. This is achieved by the decrease of the angular acceptance of the second crystal due to its asymmetrically cut surface. The asymmetry factor $b = sin(\theta_B + \alpha)/sin(\theta_B - \alpha)$ ($\alpha$: angle between crystal surface and lattice planes) was ~ 8 at the wavelength $\lambda$=0.154 nm used in our experiments. The first as well as the third crystal is cut parallel to the (111) lattice planes. Whereas crystal I and II reflect in the first order, the third crystal is set at the (333) reflection. The intensity measured by means of a NaI(Tl)-scintillator behind the third crystal is normalized to the intensity on the first crystal, monitored by the total photoelectron yield from a carbon foil placed in front of it. By means of the slit S 1 (fig. 5) the total power load on the first crystal was changed. The monochromator is operating in vacuum. The reflection curve of the first crystal was measured by changing $\theta$ (fig. 5). Crystal II and III are fixed during the measurement.

Two different cooling schemes of the first crystal were tested :

1. The crystal is mounted in a copper holder which is pressed against a copper support containing two water channels for cooling. (fig. 6a). Further, this cooling scheme will be called indirect cooling (i).
2. In the direct cooling scheme (d) the crystal is pressed directly onto the cooled copper support (fig. 6b)

## 4. Discussion

In figure 7 typical rocking curves are shown measured during one run of DORIS for the 5mm thick Ge crystal. Whereas the angular shift of the curves results from the change of the maximum temperature in the irradiated region the width and the shape of the curves is determined by the temperature distribution at the crystal surface and its bending, respectively. From figure 7 it follows immediately that the temperature profile changes with decreasing stored current.The profile becomes flatter resulting in a decrease of the FWHM of the reflection curve. The FWHM is approximated by

$$\omega^G = ((\omega^P)^2 + (\omega^E)^2 + (\omega^L)^2 + (\omega^D)^2)^{1/2} \quad , \tag{12}$$

were $\omega^P$ is the Darwin width of the perfect crystal. The value of $\omega^D$ (equ.(10)) amounts to $< 1$ second of arc and is negligible compared to $\omega^E$ and $\omega^L$ in our case. The values of $\omega^E$, $\omega^L$ and $\omega^G$ calculated for DORIS currents of 20 and 30 mA for both 5 and 1 mm thick crystals are listed in table II. They are in good agreement with the FWHM of the measured curves which are for the 5 mm thick crystal 28.5 sec. of arc at a beam current of 33 mA and 21 sec. of arc at 22 mA, respectively (fig. 7). The decrease of $\Delta$T with decreasing DORIS current results in both a larger radius of curvature of the crystal and a decrease of the lattice spacing. This leads to narrower rocking curves with decreasing DORIS-current (see Table II). Moreover, a change in intensity causes a change $\Delta\tau$ of the average temperature. This results in an angular shift $\Delta\theta^S$ which can be calculated with an equation analogous to equation (7). Taking $\Delta\tau \sim 20$ K measured by the infrared camera for a DORIS current change from ~30 to 20 mA, we obtain $\Delta\theta^S \sim 8$ sec. of arc for the five millimeter thick crystal. from infrared measurements. The discrepancy between this value and the measured shift $\Delta\theta^S_{exp} \sim 15$ sec. of arc (fig. 7) may be explained by small vertical shifts of the beam during one run. Due to the bending of the crystal this leads to an additional angular shift of the rocking curve.

With the values of table II we conclude that the decrease of the rocking curve width by the use of thinner crystals is only caused by its smaller expansion. The bending of the crystal does not strongly depend on its thickness, due to the high photoelectric absorption coefficient of germanium (see fig.1). Figure 8 gives an overview of the measured FWHM for the two different cooling schemes and crystal thicknesses versus the mean crystal temperature, measured by a thermocouple located outside of the irradiated region. It should be mentioned that the 1 mm thick crystal was of smaller size than the thicker one. Therefore the temperature measured by the thermocouple is higher due to its smaller distance from the irradiated region (fig. 8). Whereas the mean temperature of the 5 mm thick crystal can be significantly lowered by the more effective direct cooling, the FWHM of the rocking curves caused by the temperature distribution inside of the crystal changes only slightly. Taking a one millimeter thick Ge crystal, the maximum temperature inside the crystal is decreased by a factor of $\sim 5$ resulting in narrower rocking curves. This is accompanied with an increase of the maximum intensity of the rocking curve by about a factor $\sim 3$ (fig. 9). As expected, the reflectivity of the crystal becomes higher due to the flatter temperature profile in the thinner crystal.



## 5. Summary

The results derived from three crystal rocking curve measurements of thermally loaded Ge (111) crystal are compared with heat load calculations. The changes of the rocking curves are due to both the thermal expansion and the overall bending of the heated crystal. The efficiency of the cooling scheme does not significantly affect the shape of the rocking curves. By use of a 1 mm instead 5 mm thick crystal the reflected maximum intensity was increased by a factor $\sim 3$. This is due to a smaller temperature gradient inside the crystal. Nevertheless, the bending of the crystal induced by the thermal load depends only slightly on its thickness. Therefore the use of thin crystal plates seems to be limited to moderate power incident on the crystal. Further experiments with ringed and grooved crystals are underway in our laboratory.

## Acknowledgements

Drs. V. Saile and G.Materlik are acknowledged for helpfull discussions. We thank R.Treusch and H.B.Peters for their help during the experiments and the performance of the finite element calculations, respectively.

References:


[1] R.T. Avery, Nucl.Instr.and Meth. 222 (1984), 146
[2] S.Mourikis, E.E.Koch and V.Saile, Nucl.Instr.and Meth. A267 (1988), 218
[3] S.Mourikis, W.Jark, E.E.Koch and V.Saile, Rev.Sci.Instrum. 60(7),1474 (1989)
[4] D.H.Bilderback, C.Henderson, J.White, R.K Smither and G.A.Forster, Rev.Sci.Istrum. 60(7),1973 (1989)
[5] E.Ziegler, Y.Lepetre, St.Joksch, V.Saile, S.Mourikis, P.J.Viccaro, G.Rolland and F.Laugier, Rev.Sci.Instrum. 60(7), 1995 (1989)
[6] R.K.Smither, G.A.Forster, C.A.Kot and T.M.Kuzay, Nucl.Instr.and Meth. A266 (1988), 517
[7] D.H.Bilderback, Nucl.Instr.and Meth. A246 (1986), 434
[8] D.H.Bilderback, D.M.Mills, B.W.Batterman and C.Henderson, Nucl.Instr.and Meth. A246 (1986), 428
[9] P.Gürtler and A.Jackson, Nucl.Instr.and Meth. 208 (1983), 163
[10] P.Gürtler, Nucl.Instr.and Meth. A246 (1986), 91
[11] J.Kalus, G.Gobert and E.Schedler, J.Phys.E6, 488 (1973)
[12] A.K.Freund, Nucl.Instr.and Meth. 216 (1983), 269
[13] G.S.Knapp and R.K.Smither, Nucl.Instr.and Meth. A246 (1986), 365
[14] A.Fukuhara and Y.Takado, Acta Cryst. A33, 137 (1977)
[15] P.Suortti and A.K.Freund, Rev.Sci.Instrum. 60(7), 2126 (1989)
[16] W.Jark, S.Mourikis, St.Joksch and V.Saile, Nucl.Instr.and Meth.A (submitted)




figure captions:

Table I : Calculated and measured maximum temperatures at the surface of the first monochromator crystal (Ge (111), 5 mm thick; $P_{tot}$: total power on first crystal, P': maximum power density, $T_{max,exp}$: experimental, $T_{max,calc}$ : calculated by finite element methods, $\Delta$ T: Temperature difference in the crystal calculated by 1-dimensional model)

Table II : Rocking curve broadening due to thermal load (details see text)

Figure 1: W1-wiggler spectrum in the orbit plane and photoelectric absorption coefficients of Si and Ge

Figure 2: Temperature difference vs. depth for 5mm thick crystals in the ROEWI monochromator at HASYLAB calculated for (a) parasitic (5.3 GeV,80mA,) and (b) dedicated (3.65GeV,100mA,) shifts of DORIS

Figure 3: Calculated surface temperature distribution in one quadrant of the first crystal in the ROEWI monochromator at the wiggler beamline W1 (DORIS parameters: 5.3GeV, 30 mA, crystal thickness: 5mm (top), 1mm (bottom), Slit S I: 10 mm x 30 mm))

Figure 4: Deformation of the 5 mm thick crystal calculated by finite element methode using the temperature distribution of figure 3.

Figure 5: Experimental layout (b: asymmetry factor)

Figure 6: Indirect (i) and direct (d) cooling schemes (C: crystal, In: In-foil, Cu: copper, $H_2O$ : water cooling)

Figure 7: Measured (1,-1,-3)-rocking curves of the first monochromator crystal (Ge (111), 5mm thick) for different electron currents with DORIS operating at 5.3GeV.

Figure 8: Comparison of the reflection width (FWHM) of 5 and 1 mm thick Ge (111) crystals, directly (d) and indirectly (i) cooled

Figure 9: Comparison of the maximum reflectivity of 5 and 1 mm thick Ge (111) crystals, directly (d) and indirectly (i) cooled

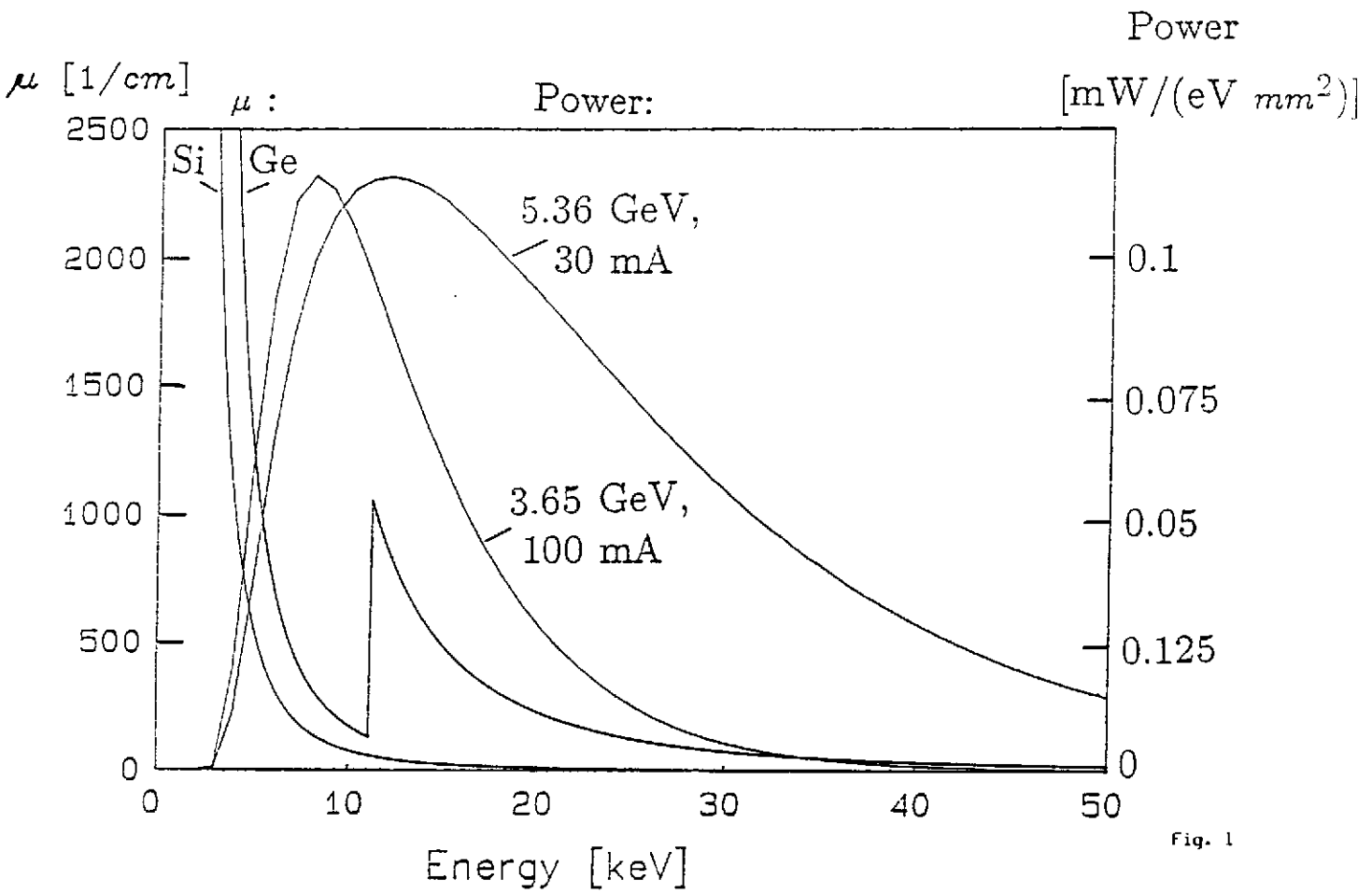


Fig. 1

Table I

| I [mA] | $P_{tot}$ [W] | P' $[\frac{W}{mm^2}]$ | $T_{max,exp}$ [K] | $T_{max,calc}$ [K] | $\Delta T$ [K] |
|---|---|---|---|---|---|
| 30 | 210 | 0.72 | 135 | 134 | 63.6 |
| 20 | 160 | 0.48 | 105 | 96 | 42.5 |

Table II

| $z_0$ [mm] | I [mA] | $\Delta T$ [K] | R [m] | $\omega^L$ [sec.of arc] | $\omega^E$ [sec.of arc] | $\omega^G$ [sec.of arc] | $\omega_{exp}$ [sec.of arc] |
|---|---|---|---|---|---|---|---|
| 5 | 30 | 63.6 | 13.6 | 15.1 | 24.3 | 33.7 | 28.5 |
| | 20 | 42.5 | 20.5 | 10.1 | 16.2 | 26.1 | 21.0 |
| 1 | 30 | 13.1 | 13.6 | 15.1 | 4.4 | 22.6 | 20.5 |
| | 20 | 8.7 | 20.5 | 10.1 | 2.9 | 20.1 | 20.5 |

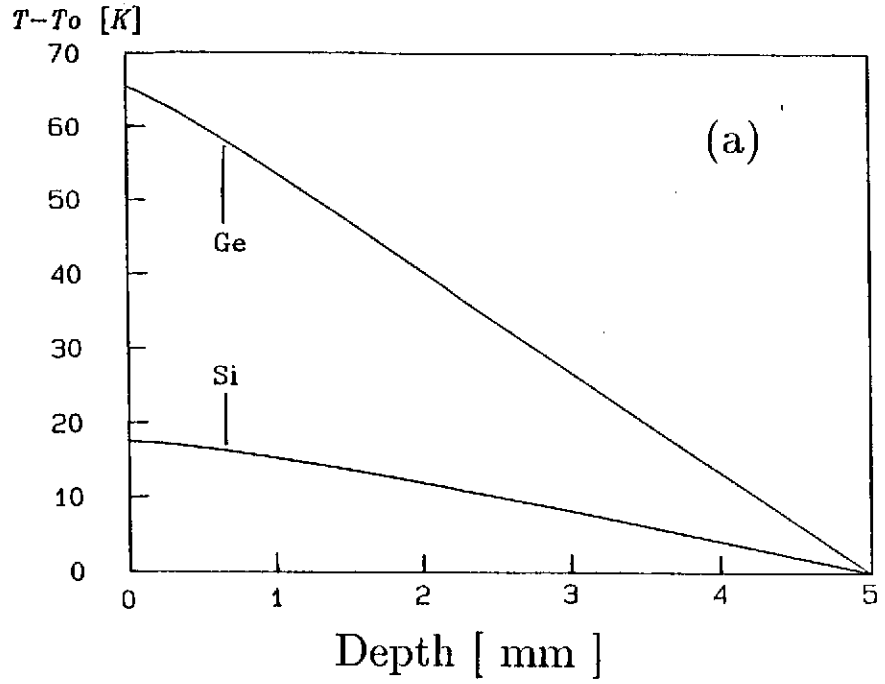
T-To [K]
70
60
50
40
30
20
10
0
(a)
Ge
Si
0
1
2
3
4
5
Depth [ mm ]

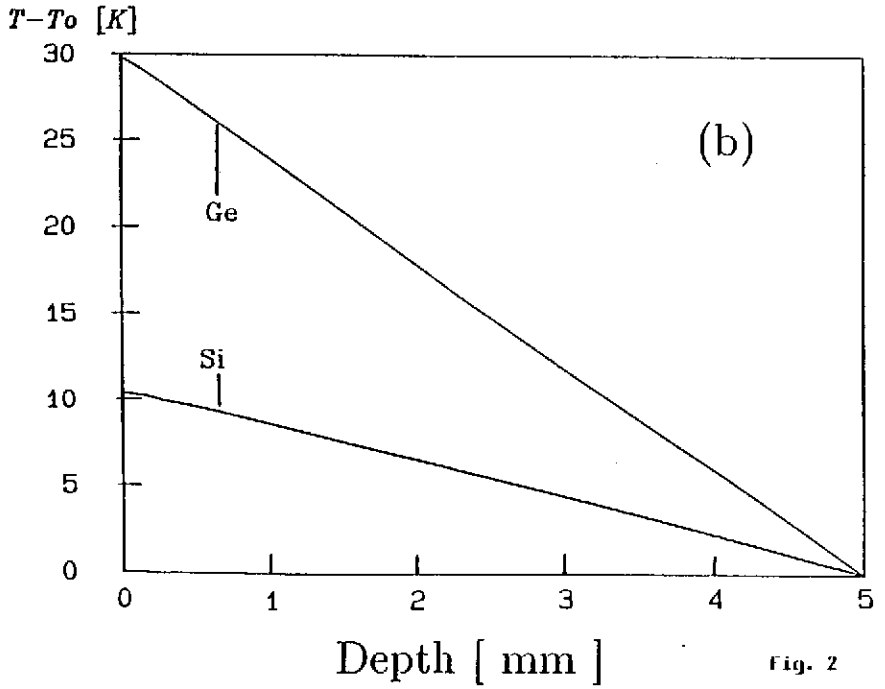
T-To [K]
30
25
20
15
10
5
0
(b)
Ge
Si
0
1
2
3
4
5
Depth [ mm ]

Fig. 2

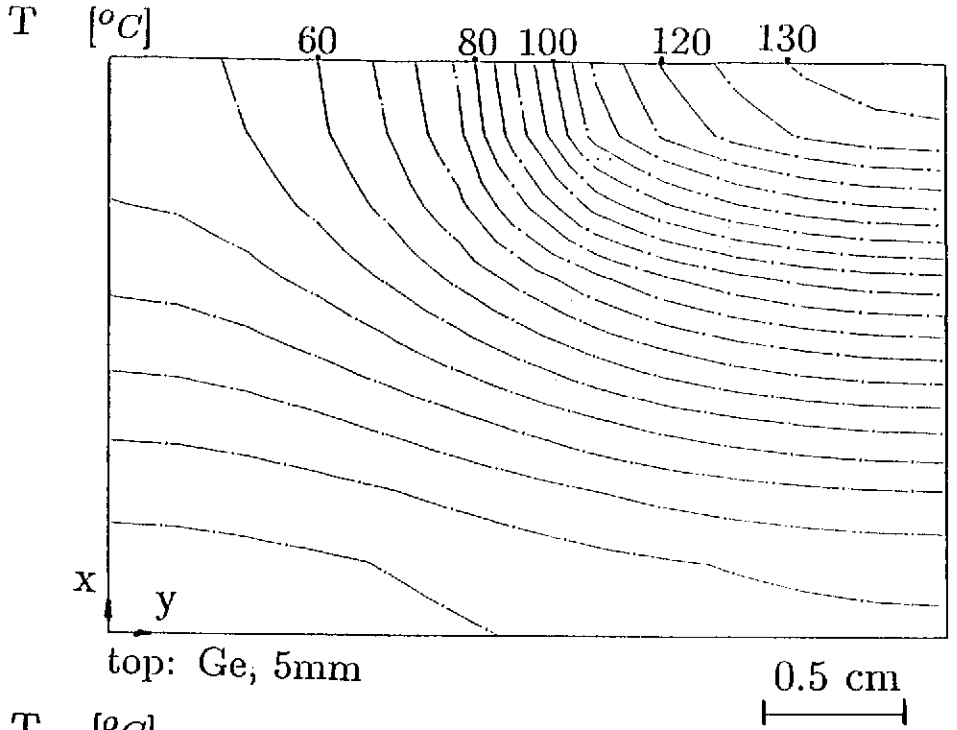
T [°C]
60
80
100
120
130
x
y
top: Ge, 5mm
0.5 cm

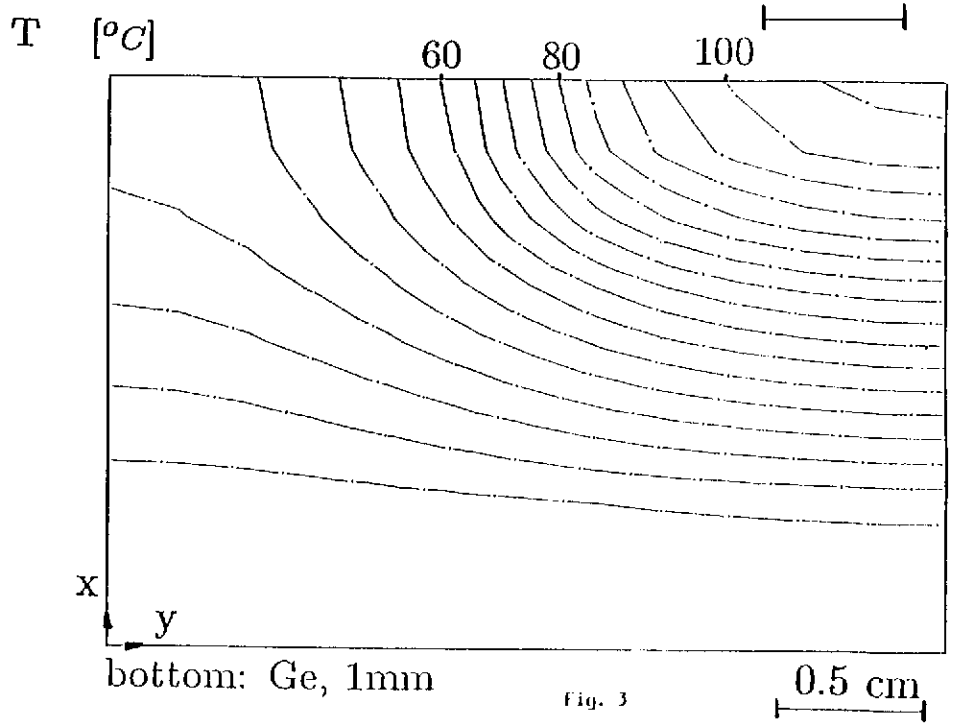
T [°C]
60
80
100
x
y
bottom: Ge, 1mm
0.5 cm

Fig. 3

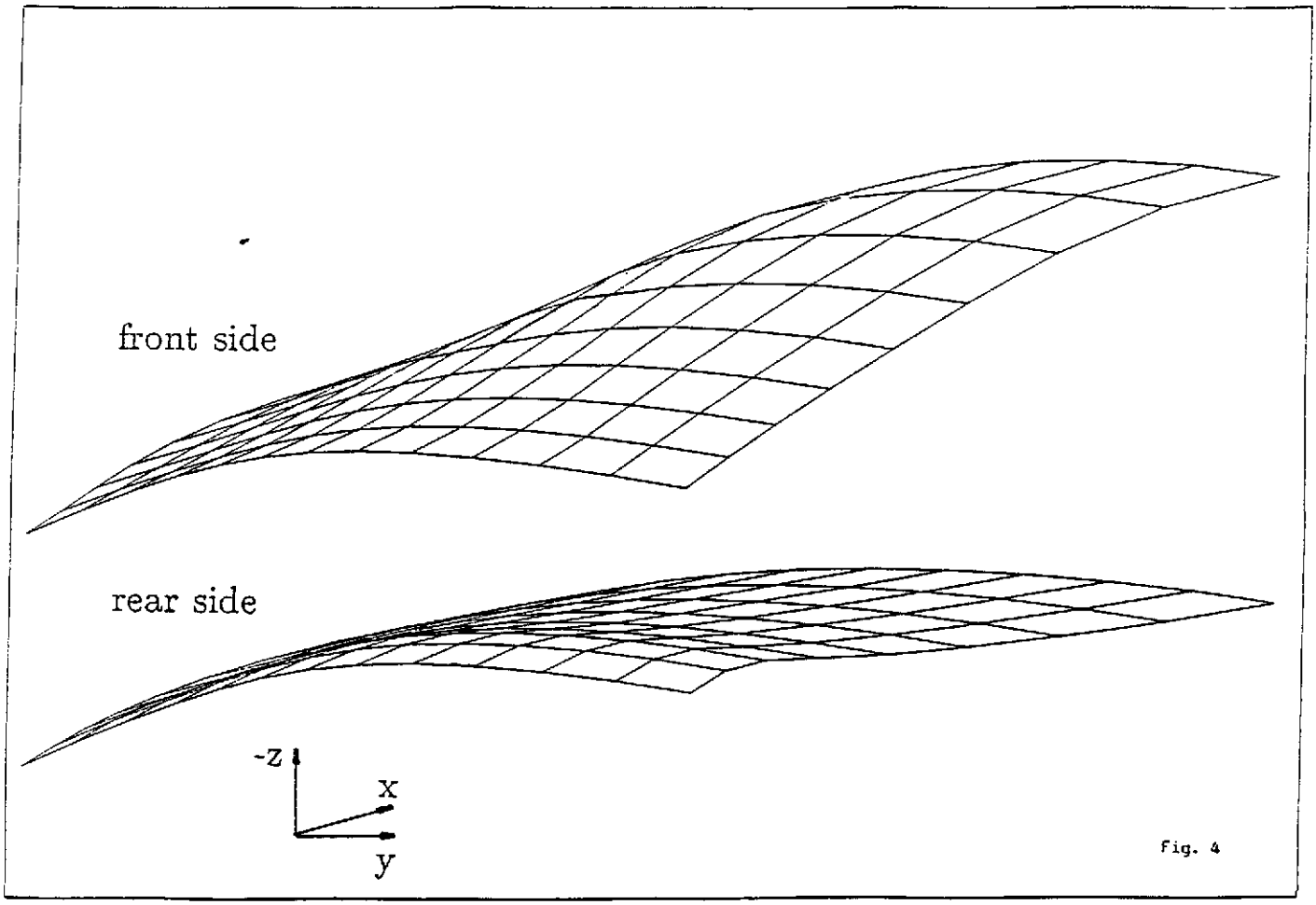
front side
rear side
-z
x
y

Fig. 4

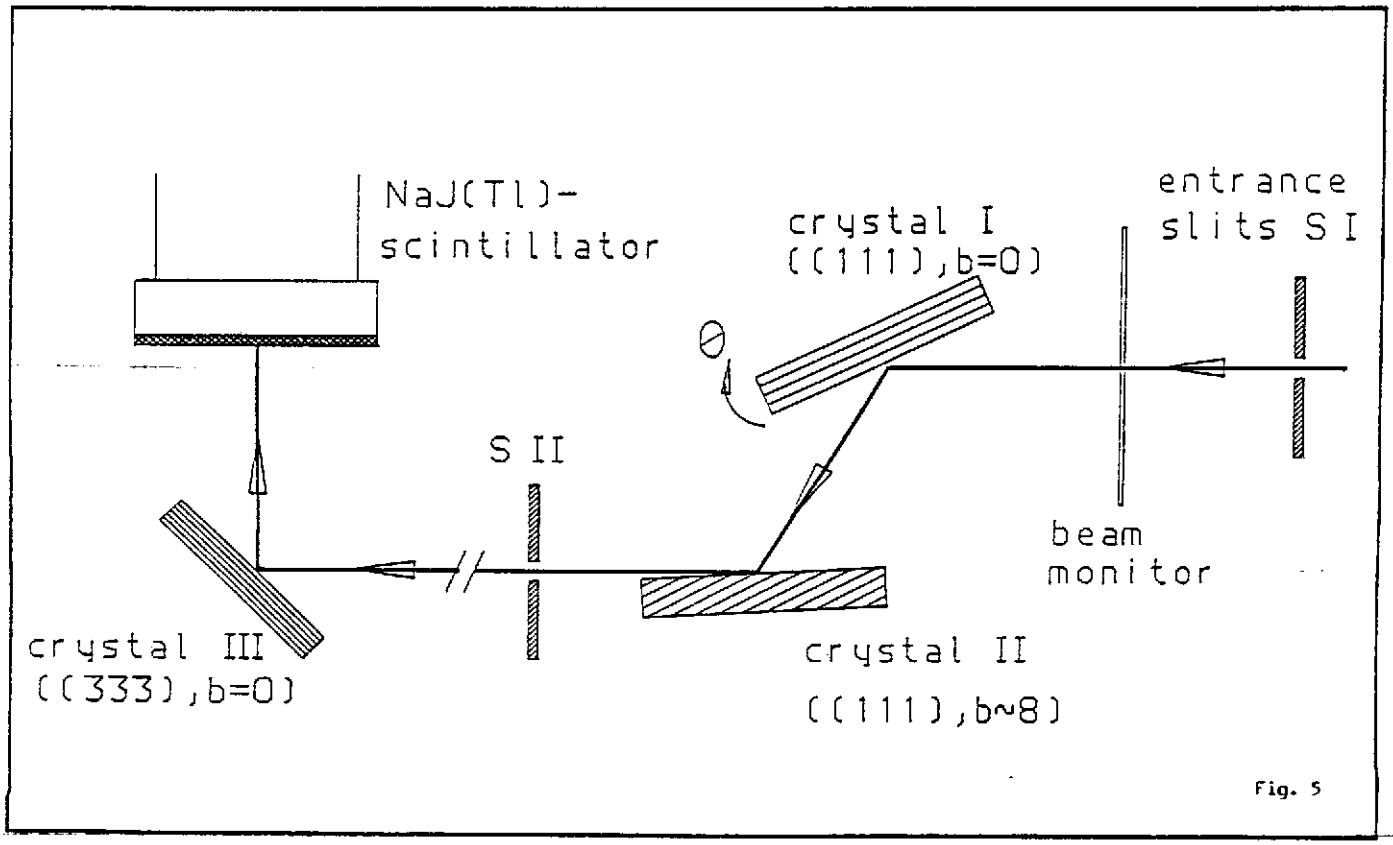
NaJ(Tl)-
scintillator
crystal I
((111),b=0)
entrance
slits SI
S II
beam
monitor
crystal III
((333),b=0)
crystal II
((111),b~8)

Fig. 5

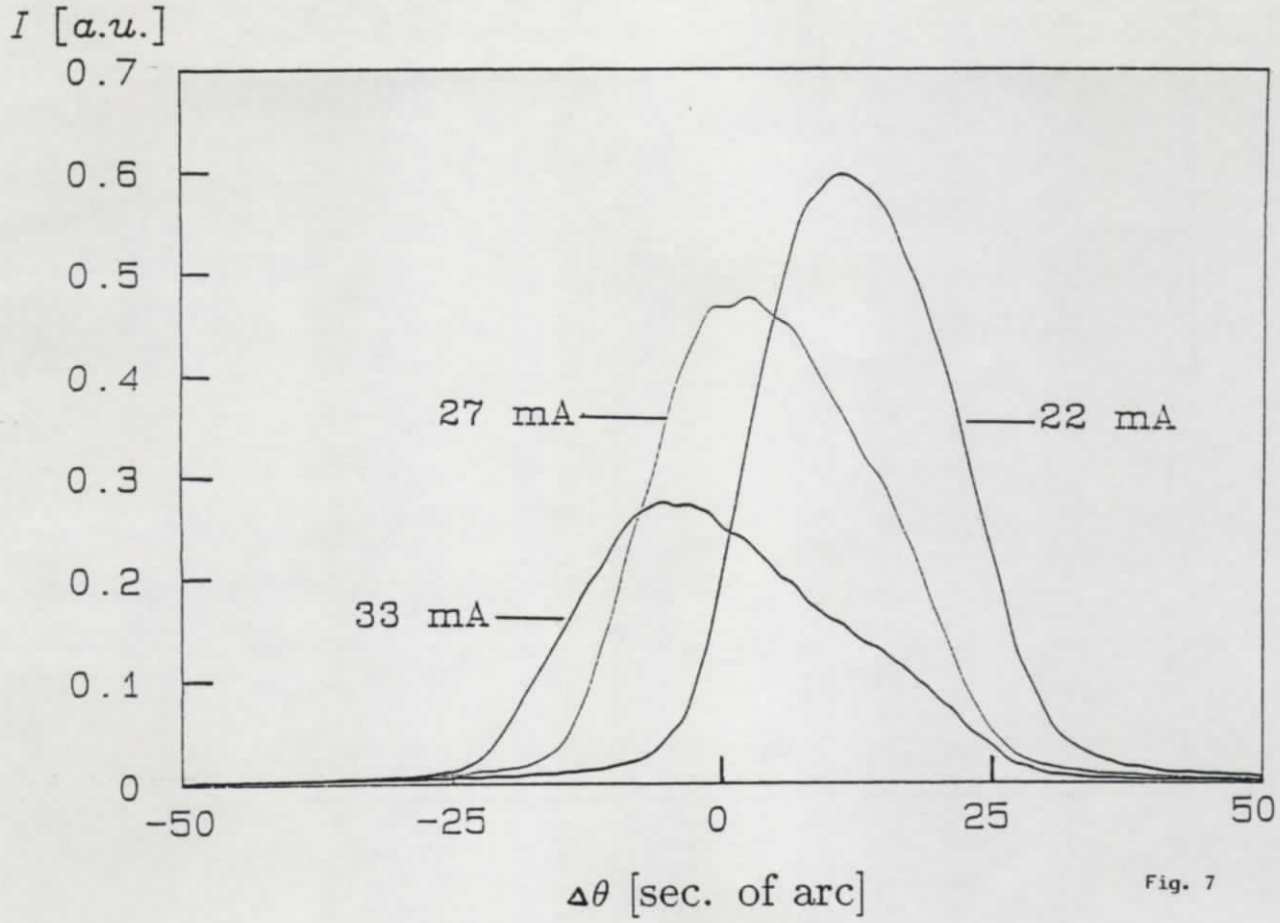
I [a.u.]
0.7
0.6
0.5
0.4
0.3
0.2
0.1
0
-50
-25
0
25
50
27 mA
22 mA
33 mA
Δθ [sec. of arc]

Fig. 7

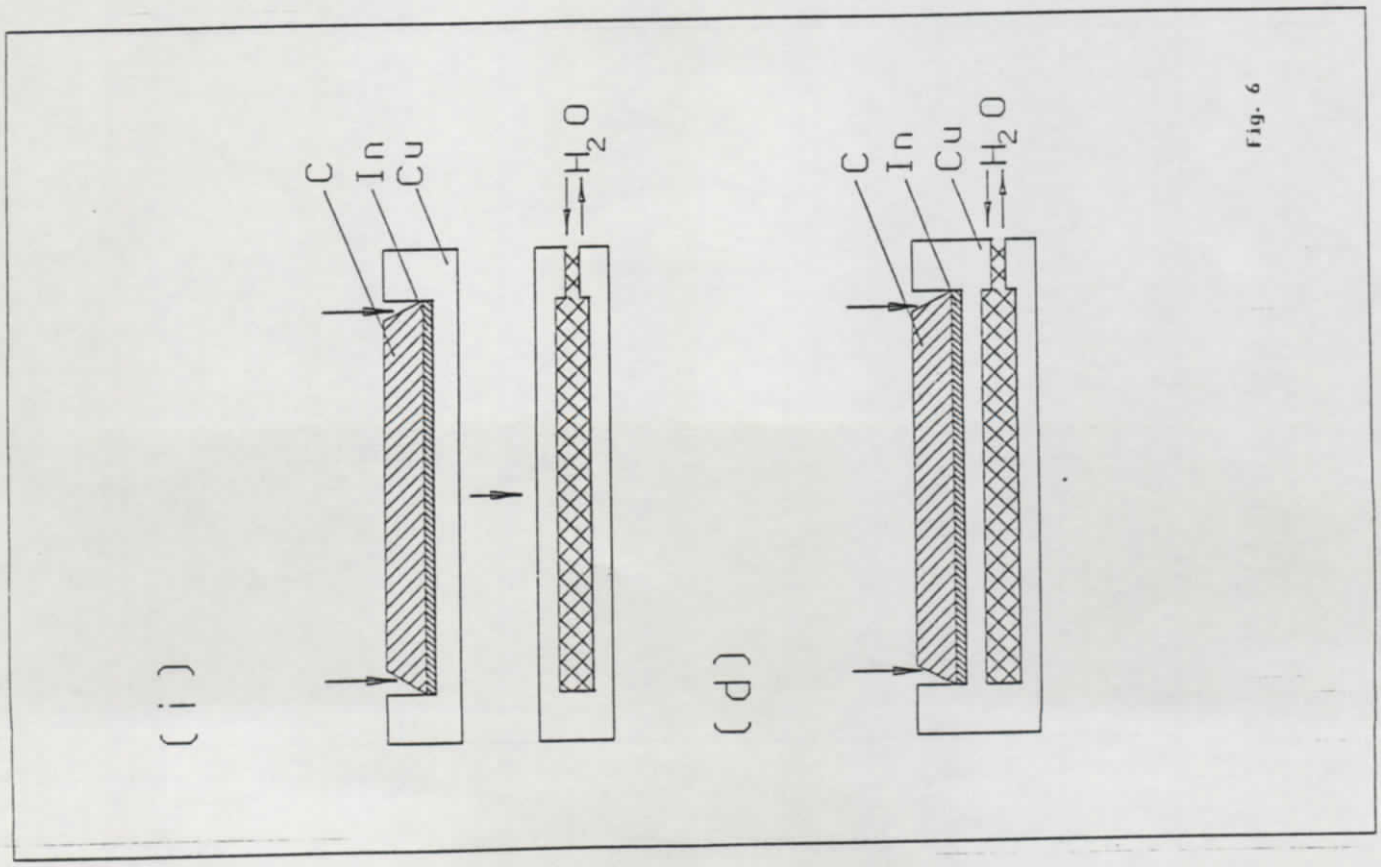
C
In
Cu
$H_2O$
(i)
(d)

Fig. 6

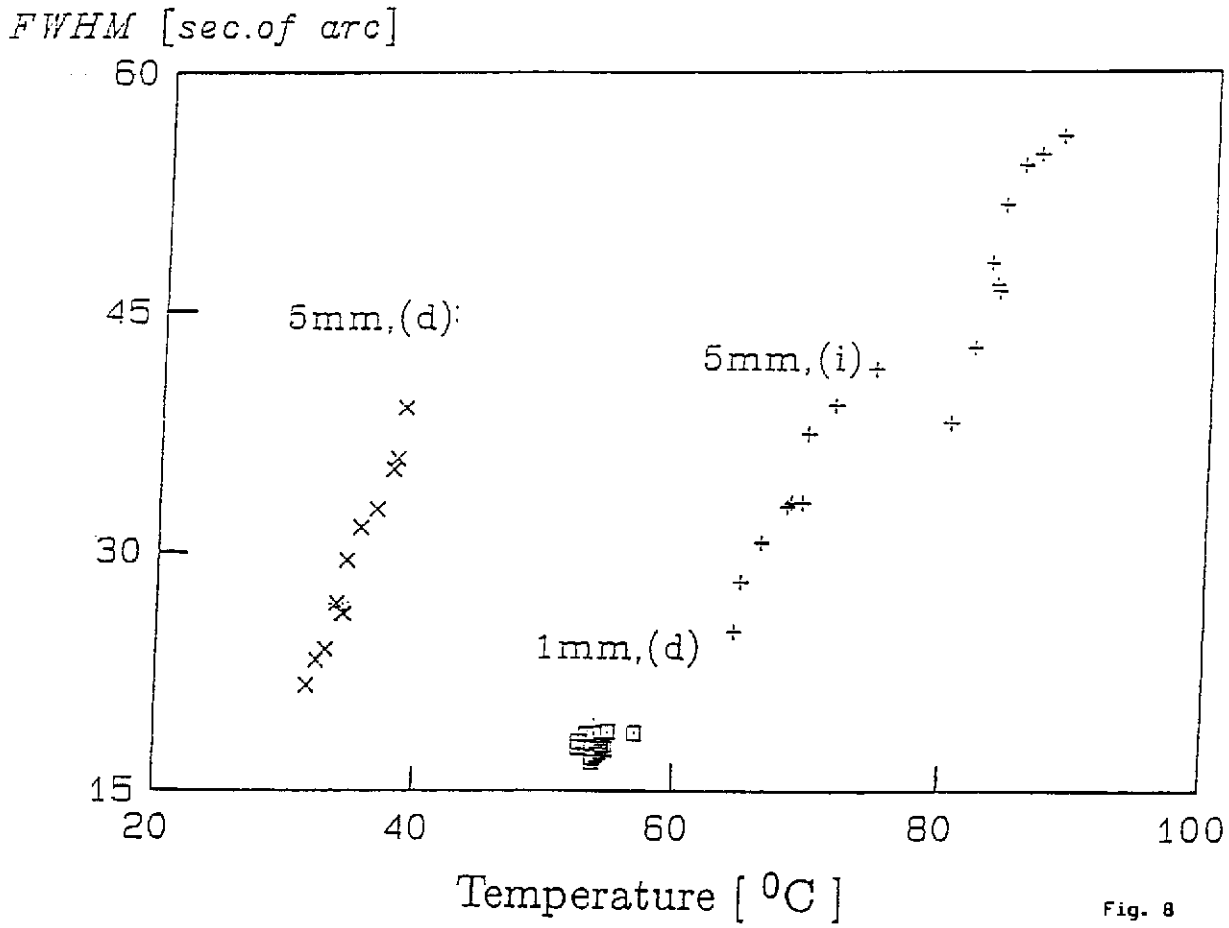
FWHM [sec.of arc]
60
45
30
15
5mm,(d)
5mm,(i)
1mm,(d)
20
40
60
80
100
Temperature [ 0C ]

Fig. 8

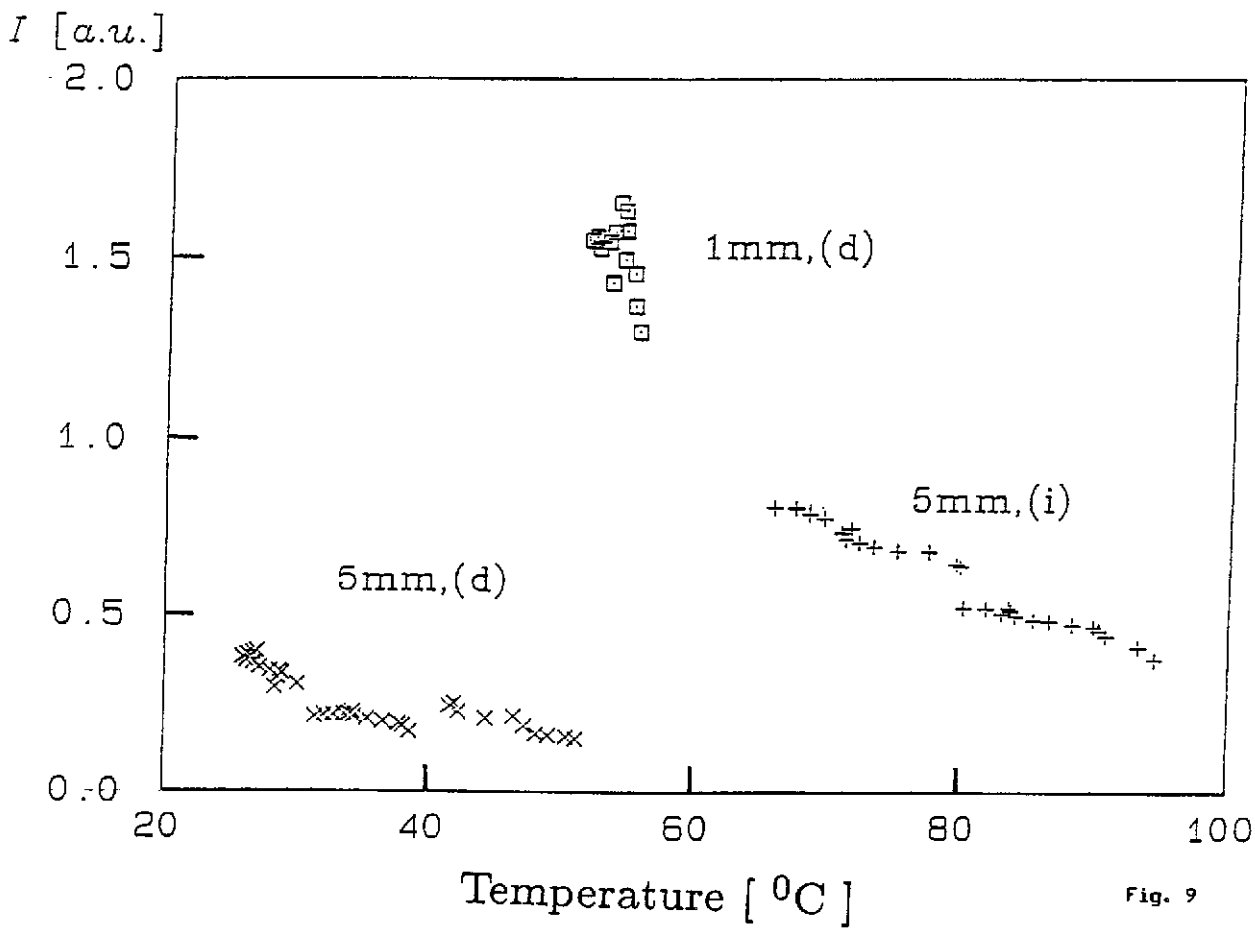
I [a.u.]
2.0
1.5
1.0
0.5
0.0
1mm,(d)
5mm,(i)
5mm,(d)
20
40
60
80
100
Temperature [ 0C ]

Fig. 9